Supporting information:

Reduced Graphene Oxide-Encapsulated Phosphorus/Carbon Composite as a Promising Anode Material for High-Performance Sodium-Ion Batteries

Gi-Hyeok Lee[a], Mi Ru Jo[a], Kai Zhang[a], Yong-Mook Kang[,a]*

[a] Department of Energy and Materials Engineering, Dongguk University-Seoul, Seoul, 100-715, Republic of Korea.

* Corresponding author E-mail: Yong-Mook Kang; dake1234@dongguk.edu

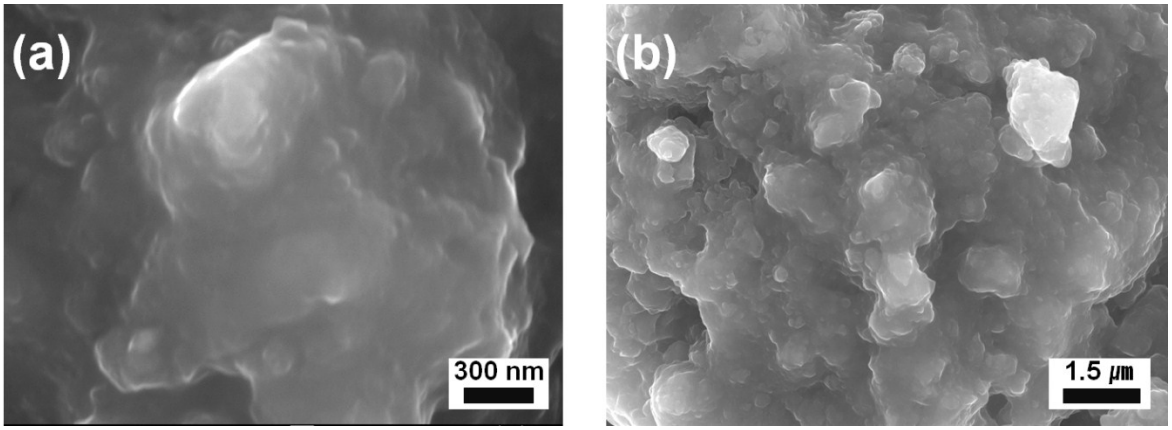

Fig. S1 SEM images of P/C@GO in different magnifications (a) x50,000 (b) x10,000

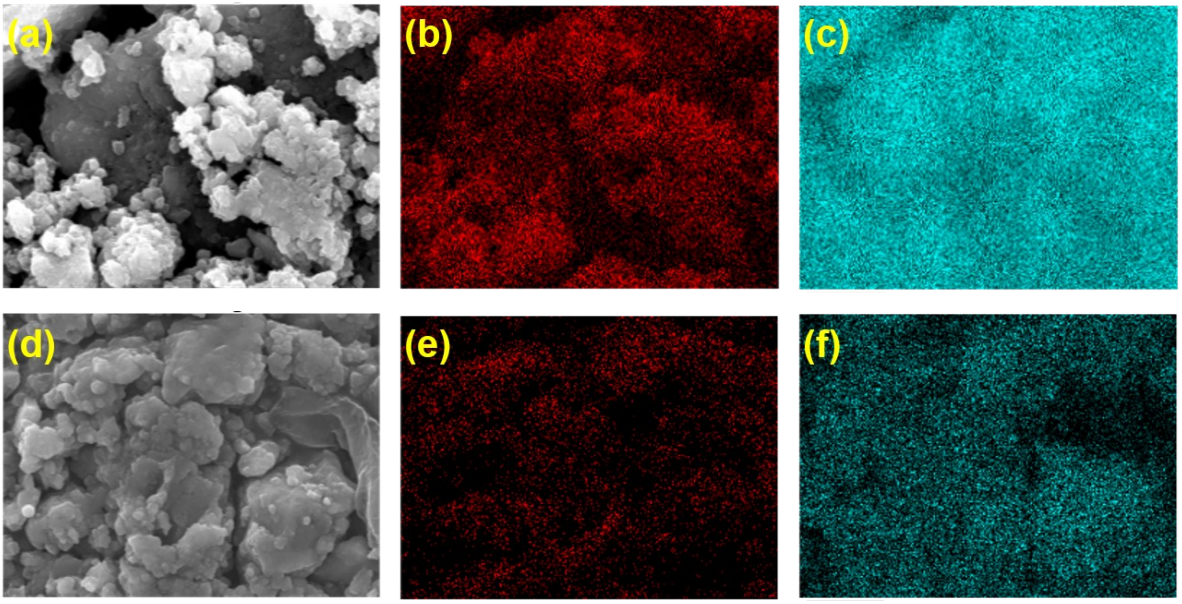

Fig. S2 Energy dispersive X-ray spectroscopy (EDS) images of P/C composite and P/C@rGO. (a, d) SEM images. (b, e) EDS images of Phosphorus. (c, f) EDS images of Carbon.

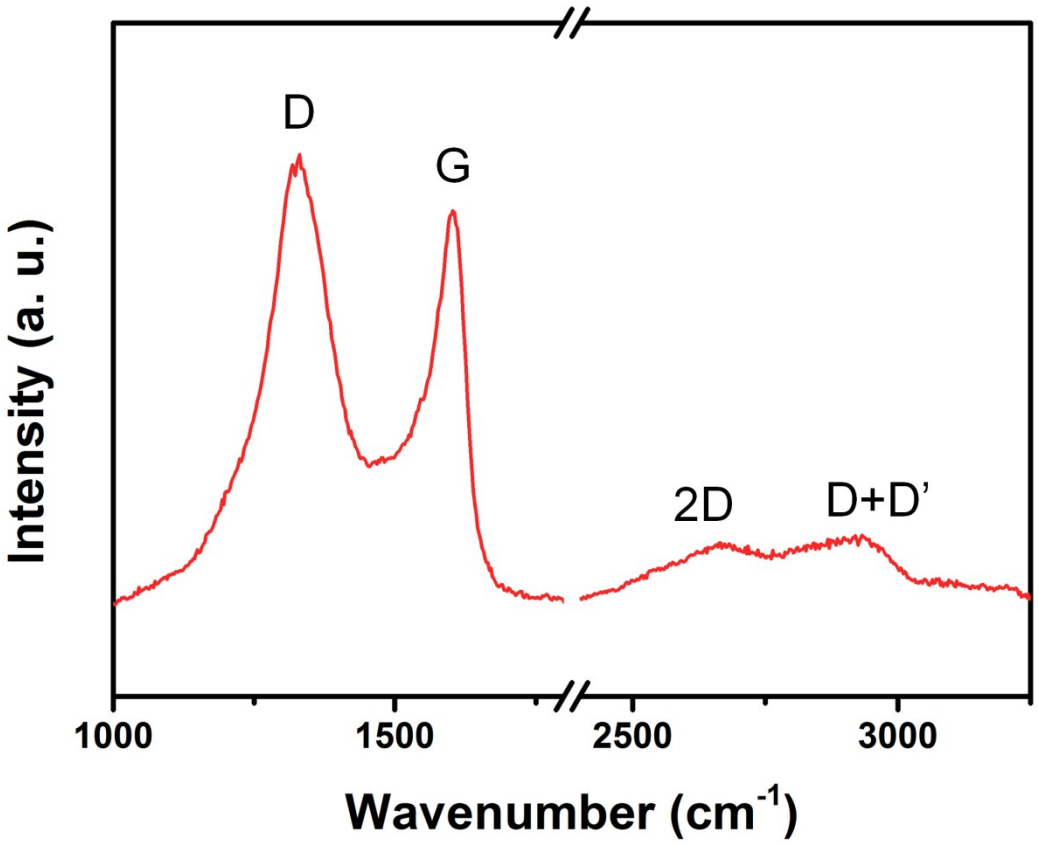

Fig. S3 Raman spectrum of P/C@rGO

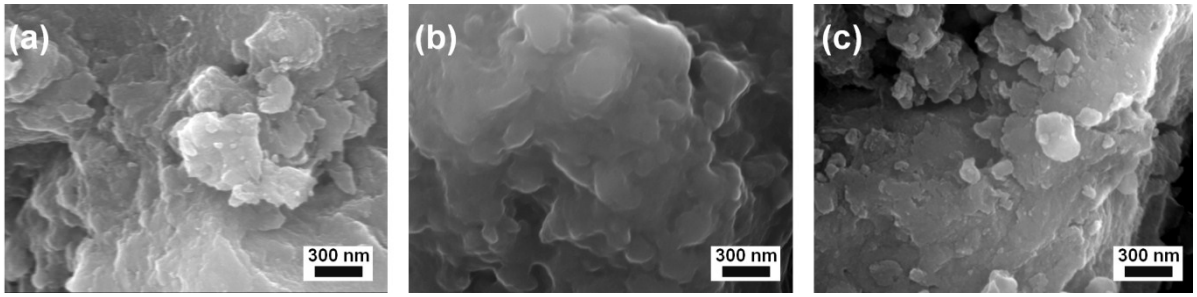

Fig. S4 SEM images of P/C@rGO with different rGO concentrations; (a) 3.0 mg/100 mL, (b) 1.5 mg/100 mL (optimum), (c) 0.5 mg/100 mL.

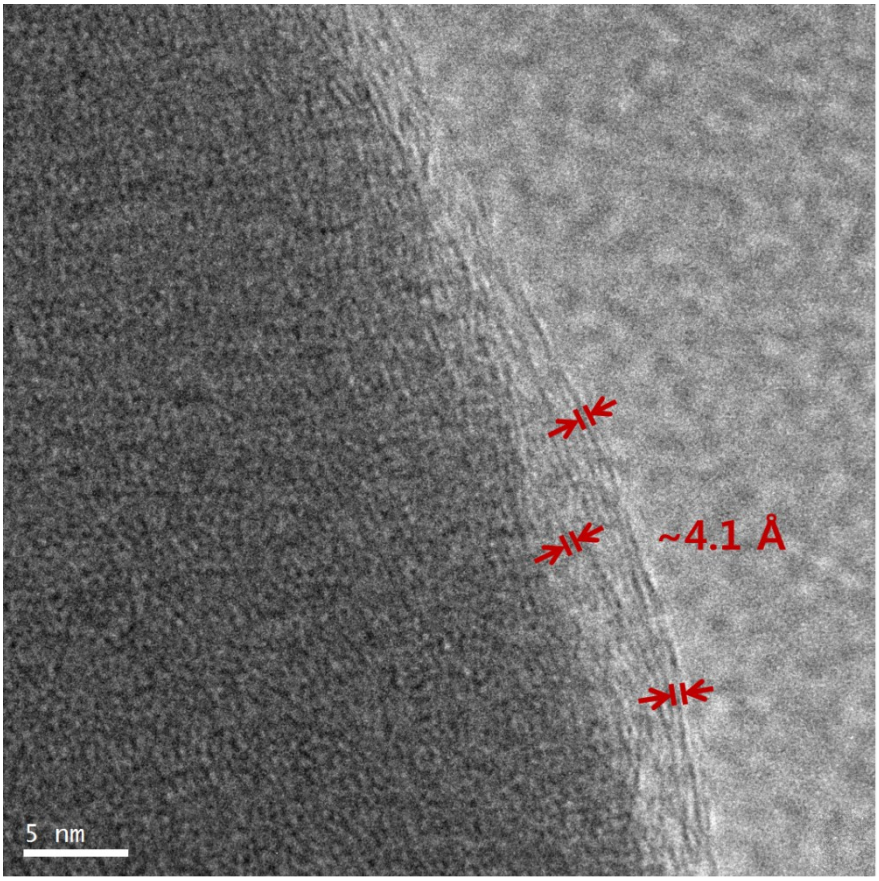

Fig. S5 D-spacing measurement of rGO coating on P/C@rGO from HR-TEM image.

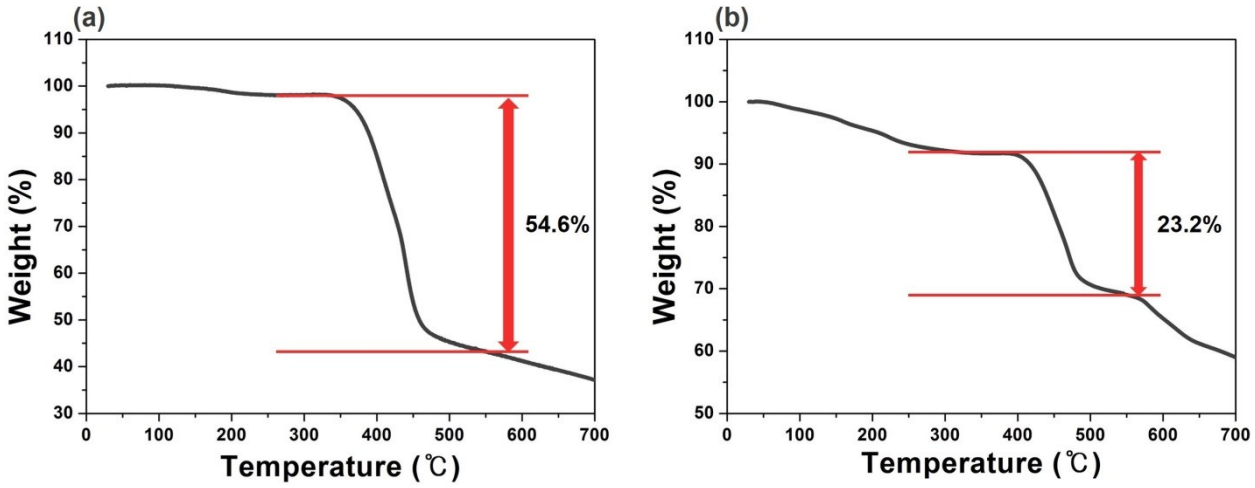

Fig. S6 Thermogravimetric analysis (TGA) of (a) P/C composite and (b) P/C@rGO.

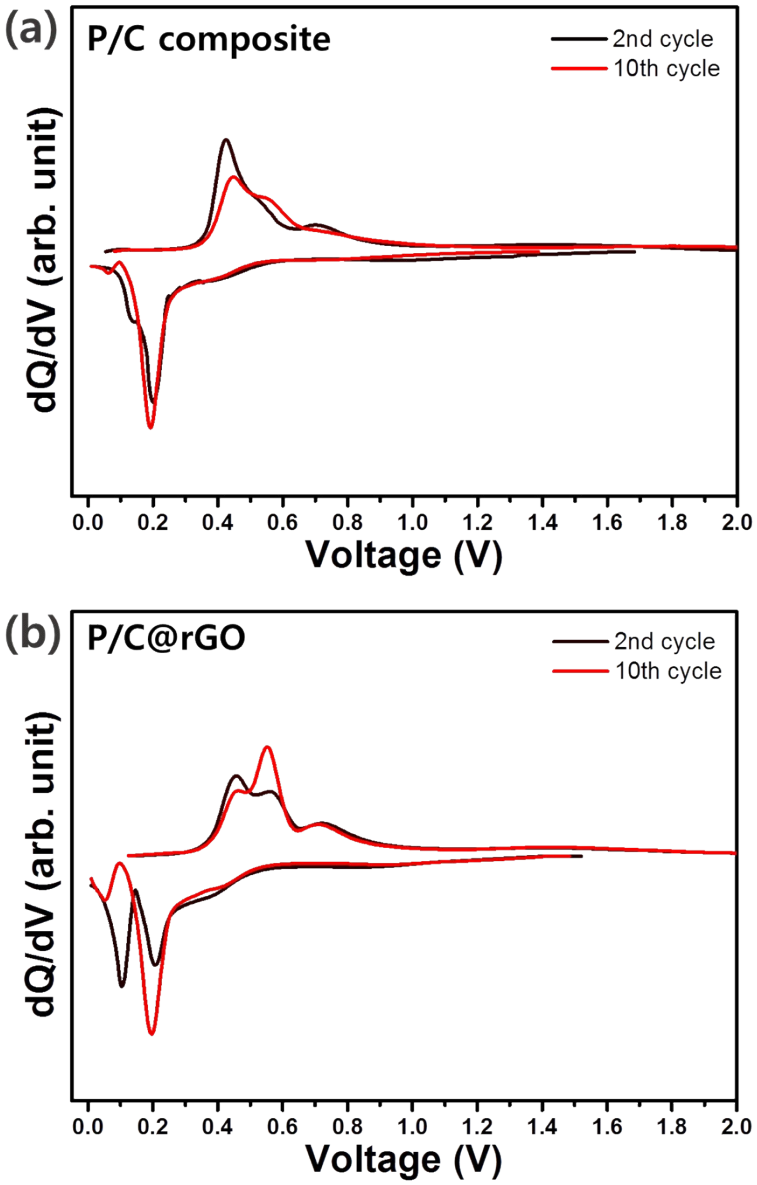

Fig. S7 dQ/dV analysis of (a) P/C composite and (b) P/C@rGO during initial 10 cycles.

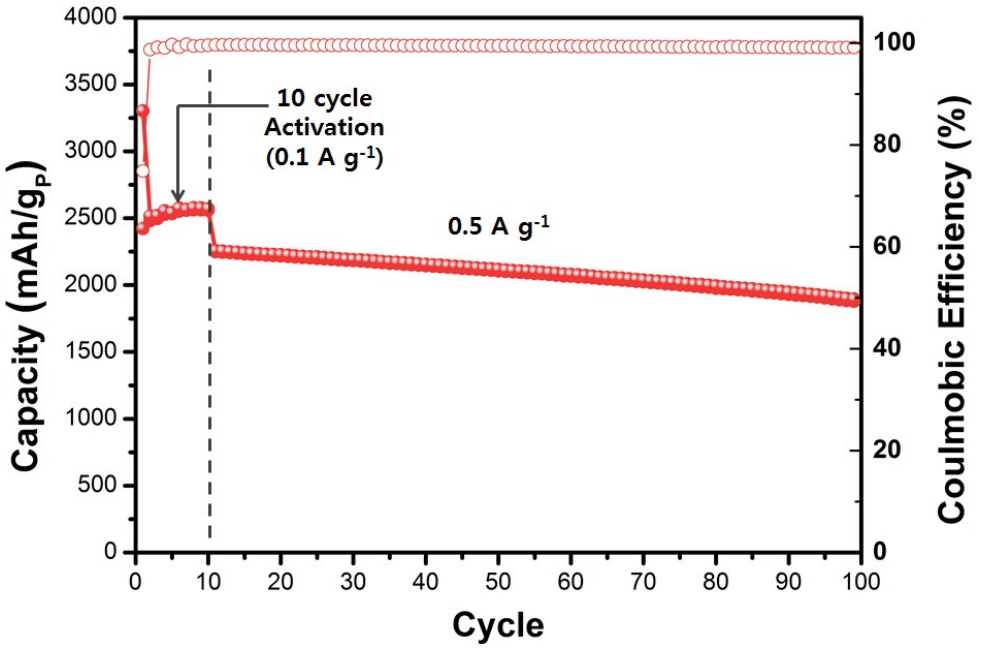

Fig. S8 Cyclic performance of P/C@rGO at a high current density of 0.5 A g^{-1}.

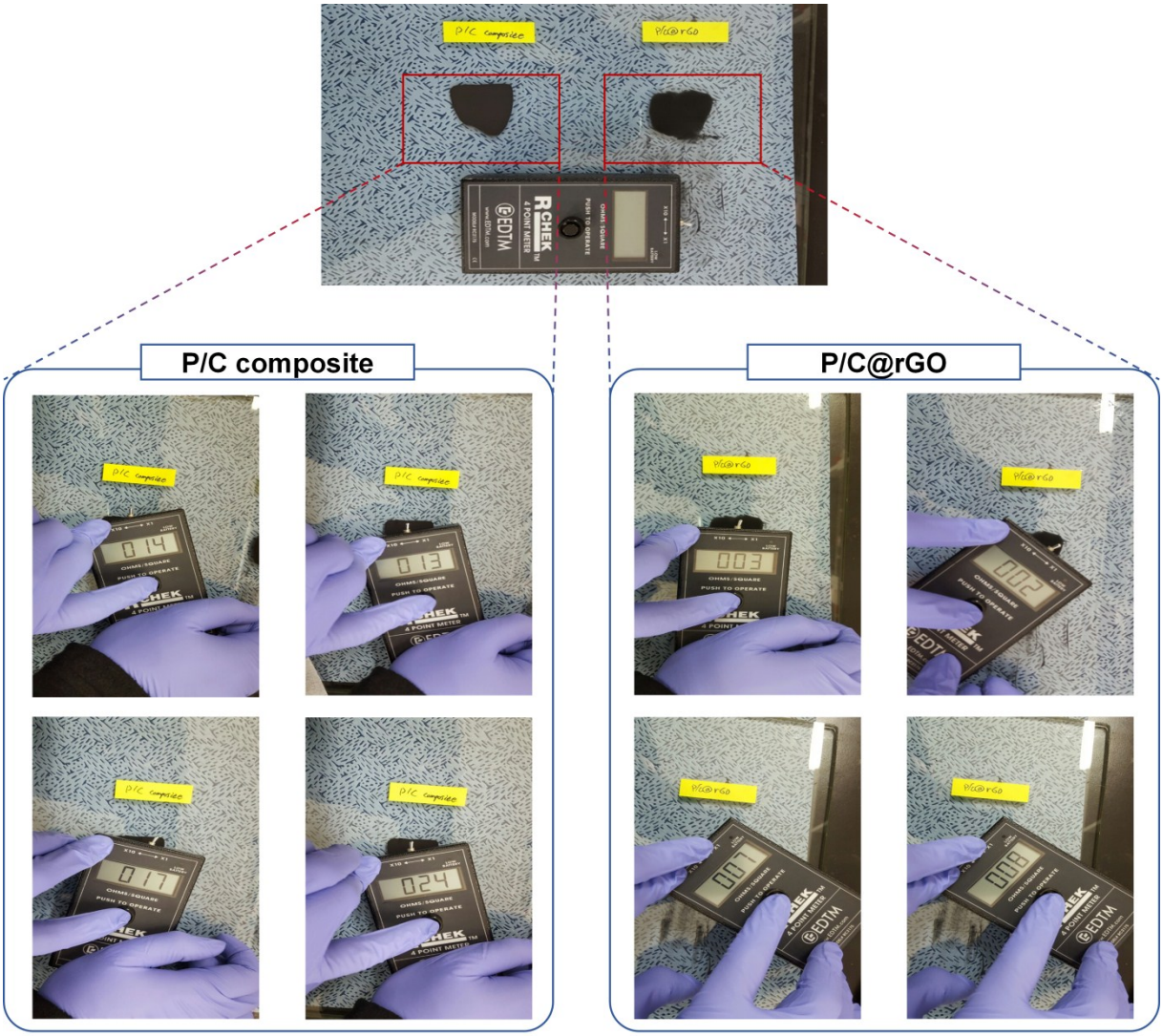

Number of Measurement	P/C composite (Ω sq^{-1})	P/C@rGO (Ω sq^{-1})
1	14	3
2	13	2
3	17	7
4	24	8
Average	17	5

Fig. S9 Sheet resistance comparison between P/C composite and P/C@rGO

$$Q_{P1} = \frac{Q_{P/C@rGO} - Q_C * W_C}{W_{P1}} \qquad \text{.................................... (1)}$$

$$Q_{P2} = \frac{Q_{P/C\ composite} - Q_C * W_C}{W_{P2}} \qquad \text{....................................}$$

(2)

Q_{P1}; Capacity contribution of phosphorus in P/C@rGO
Q_{P2}; Capacity contribution of phosphorus in P/C composite
W_{P1}; Weight ratio of phosphorus in P/C@rGO
W_{P2}; Weight ratio of phosphorus in P/C composite
Q_C; Specific capacity of Super P in P/C composite
W_C; Weight ratio of Super P in P/C composite

Table S1 Calculation formulae for capacity normalization

Active materials	Reversible Capacity (mAh g_P^{-1}) / Retention rate	Reversible capacity (mAh $g_{P/C}^{-1}$)	Reference
P/Super P	1142 at 140th cycle (100 mA g^{-1}) / 56%	800 at 140th cycle (100 mA g^{-1})	11
P/CNT	800 at 20th cycle (60 mA g-1) / 28%	500 at 20th cycle (60 mA g^{-1})	17
P/Super P	1800 at 30th cycle (50 mA g-1) / 93%	1260 at 30th cycle (50 mA g^{-1})	18
P/Graphene stack	1700 at 60th cycle (100 mA g^{-1}) / 95%	-	19
P/3D-C	2500 at 160th cycle (200 mA g^{-1}) / 88%	900 at 160th cycle (200 mA g^{-1})	20
P/C@rGO	2015 at 100th cycle (100 mA g^{-1}) / 95%	500 at 100th cycle (100 mA g^{-1})	This work

Table S2 Comparison of reversible capacities of different P electrodes for SIBs.

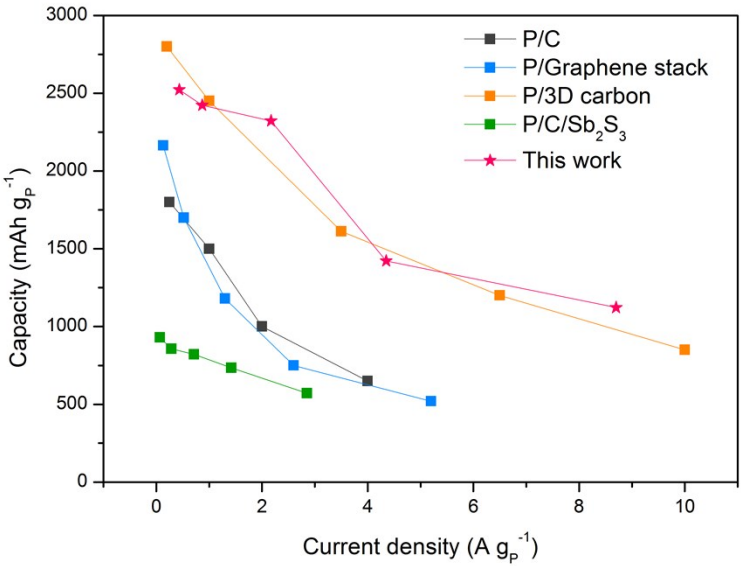

Fig. S10 Rate capability comparison among different P electrodes for SIBs.

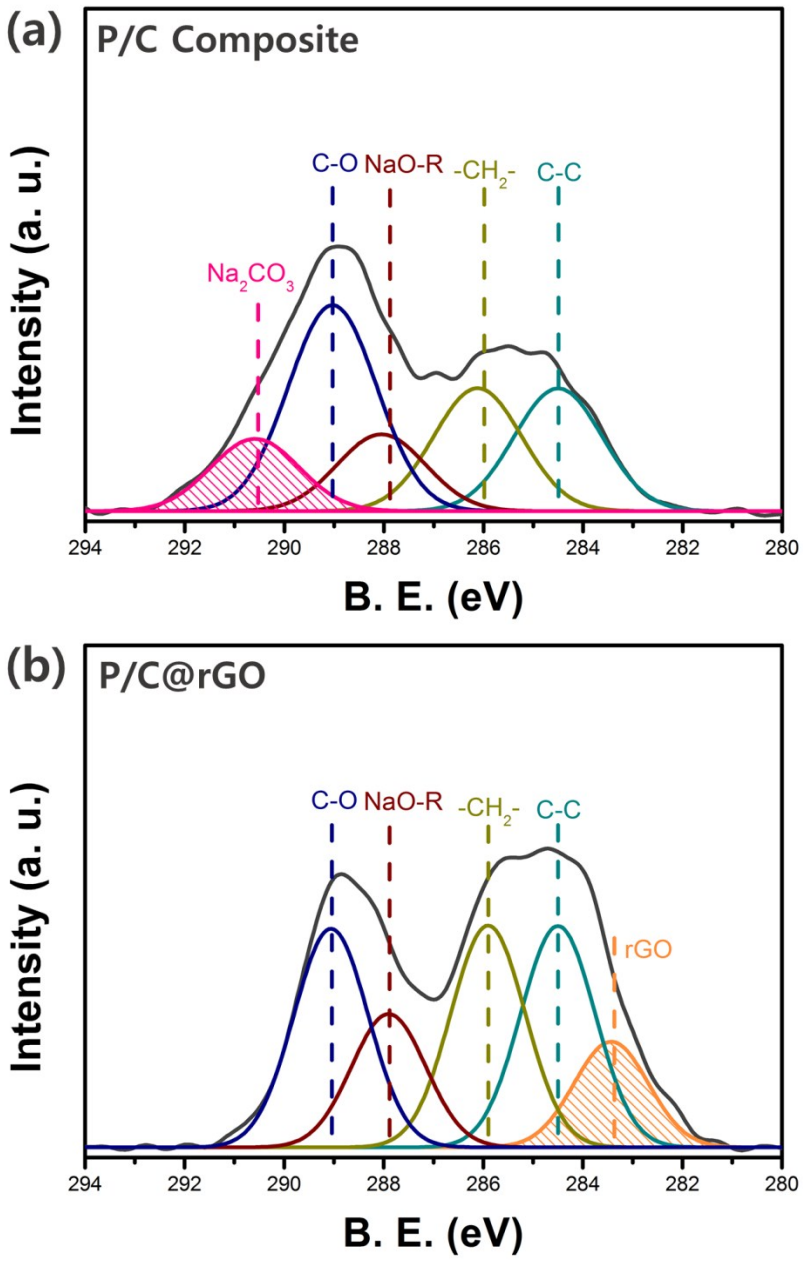

Fig. S11 Deconvolution of C 1s spectra after initial discharge to 0.01 V

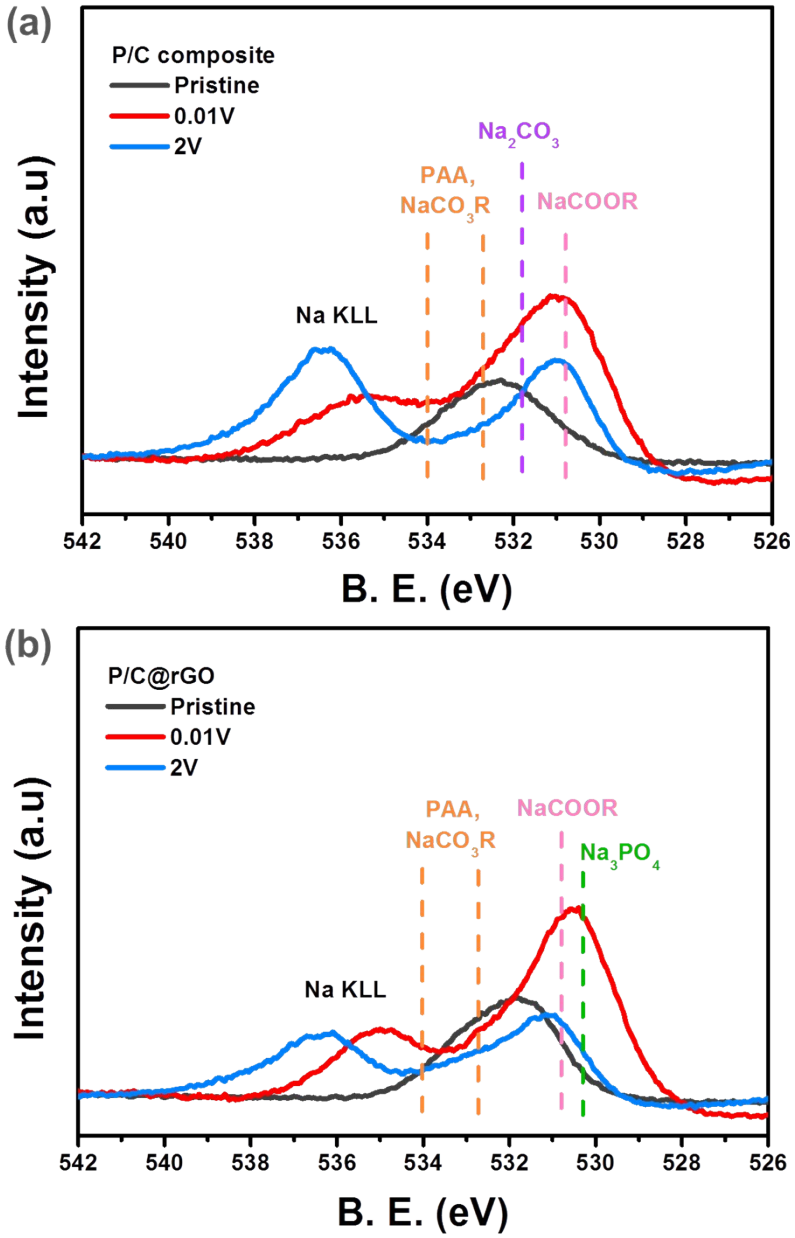

Fig. S12 O1s XPS spectra of (a) P/C composite and (b) P/C@rGO during 1st cycle.

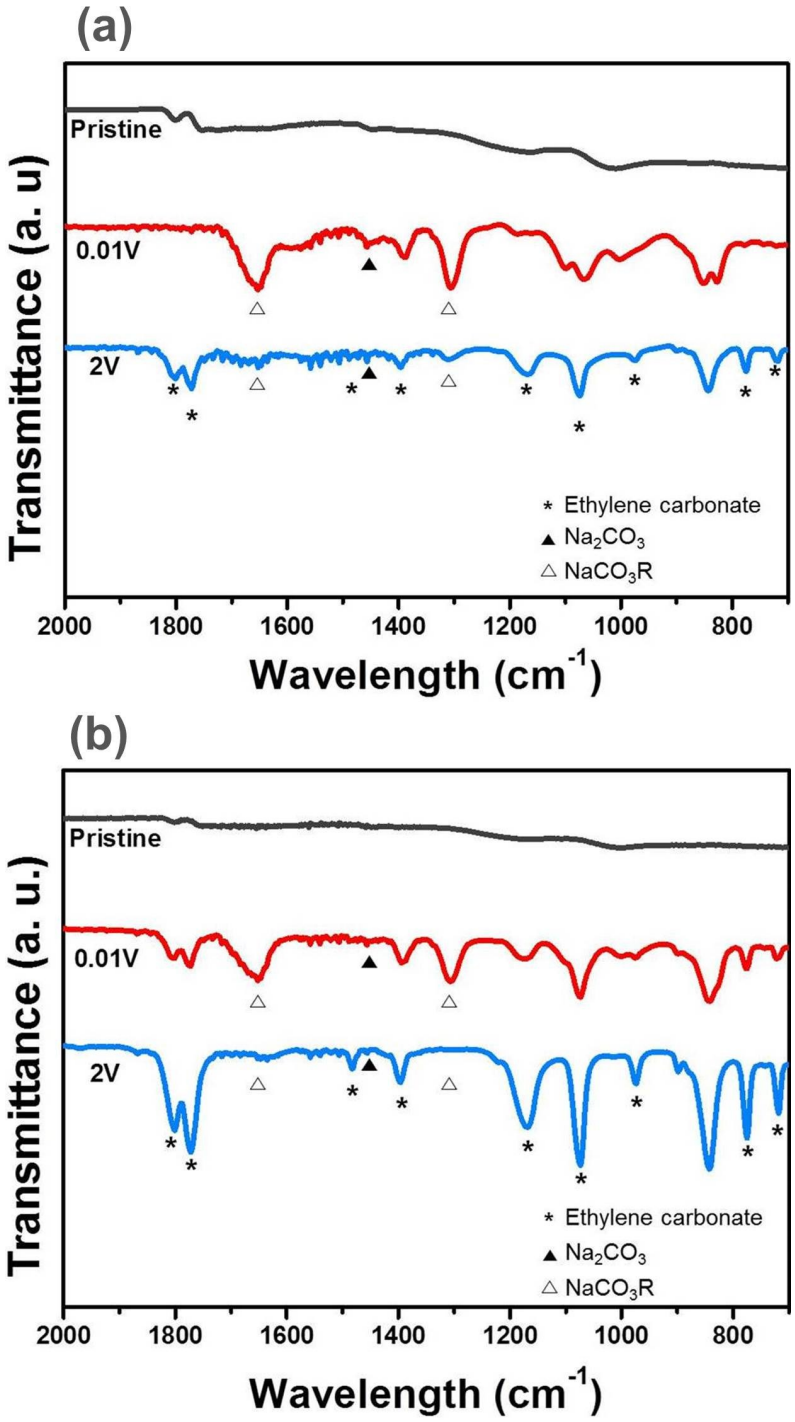

Fig. S13 Ex-situ FT-IR spectra of (a) P/C composite and (b) P/C@rGO.

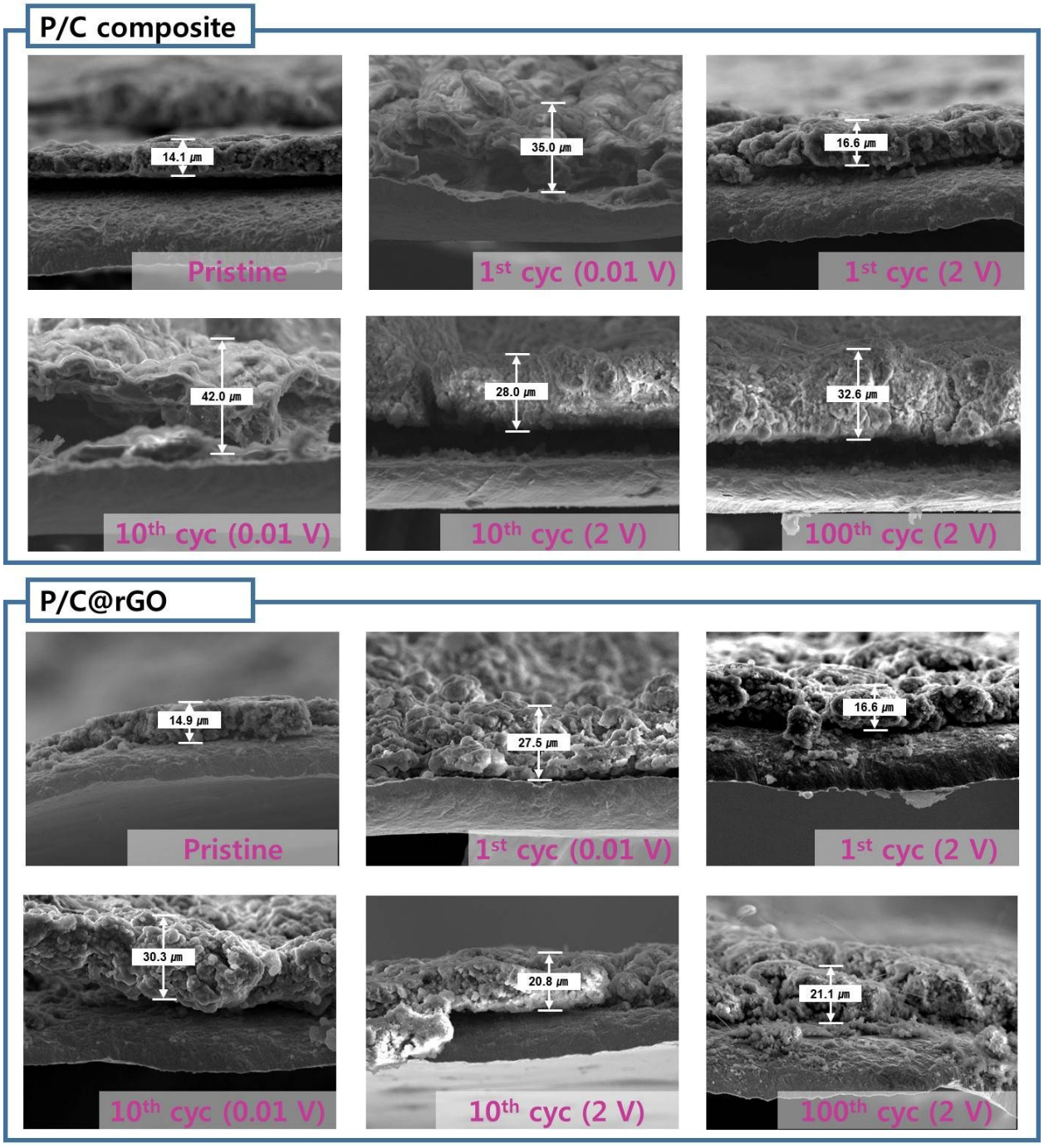

Fig. S14 Cross section SEM images of P/C composite and P/C@rGO electrodes during cycling.